AIChE

Numerical Simulation of Liquid Absorption in Paper-Like Swelling Porous Media

Reza Masoodi, Hua Tan, and Krishna M. Pillai
Laboratory for Flow and Transport Studies in Porous Media, Dept. of Mechanical Engineering, University of Wisconsin-Milwaukee, Milwaukee, WI 53211

DOI 10.1002/aic.12759
Published online September 26, 2011 in Wiley Online Library (wileyonlinelibrary.com).

The work is built on a previous research by Wiryana and Berg, in which wicking into four wet-formed paper stripes, consisting of cellulose fibers and four different percentages of the powdered carboxymethyl cellulose (CMC) superabsorbent, was studied experimentally. Because of the swelling of cellulose fibers and CMC powder on contact with water, the wicking was accompanied by a swelling of the matrix. A finite element/control volume (FE/CV)-based computer program is used for the first time to model the wicking in such swelling porous medium. The simulation used a novel form of continuity equation, which included the effects of liquid absorption and matrix swelling, in conjunction with the Darcy's law to model the single-phase flow behind a clearly defined liquid-front. A new method of estimating the time-varying permeability of the paper, based on the absorbed liquid-mass vs. time plots, is also proposed. Later, this time-dependent permeability is used in the numerical simulation to change the permeability in elements behind the moving liquid-front as a function of the time that the element has been wetted by the liquid, since the passage of the liquid-front. The numerical prediction of the wicking-front location as a function of time compares well with the reported experimental data.
 AIChE J, 58: 2536–2544, 2012
Keywords: swelling, absorption, permeability, wicking, Darcy's law, finite element method, Washburn equation, imbibition, paper

Introduction

In a previous article by Masoodi and Pillai,[1] a method to improve the predictions of liquid absorption in paper-like swelling porous media was presented, in which the flow behind a clear flow-front was assumed to be fully saturated, and where the Darcy's law and continuity equation for the single-phase flow behind the front were used as the governing equations. The continuity equation was modified to include the effects of swelling and liquid absorption in the form of two right-hand-side terms for the rate of porosity change and a sink effect.[1,2] The global values for the permeability throughout the wet porous medium were considered after neglecting its local variations.[1] Ignoring of the spatial dependence of the permeability and porosity simplified the governing equations, and turned them into an ordinary differential equation that could be solved analytically. However, this assumption, though it simplifies the governing equations, reduces the accuracy of the model.[1,2]

Another approach to model wicking is the Lucas–Washburn equation, which can be applied to one-dimensional (1-D) flows in simple geometries.[3,4] The swelling effect leads to an error, if the conventional Lucas–Washburn equation is used to predict the wicking rate in swelling porous media.[5] Therefore, Schuchardt and Berg[6] modified the Lucas–Washburn equation for application in some paper-like swelling materials, where the pore radii in the deforming porous medium decrease linearly with time as a result of the swelling. However, as observed in the experimental study published by Wiryana and Berg,[7] this assumption is not always accurate.

In general, the Darcy's law based approach is a better approach compared with the Lucas–Washburn based models, as the former can be extended to the 2-D and 3-D wicking flows.[8,9] However, in the case of complex wick-geometries, the analytical solution of the Darcy's law based governing equations may not be possible.[10] However, the advantage of the Darcy's law based approach is the possibility of using numerical simulations for predicting wicking in complex geometries.[9] Among the different numerical methods, the finite element method (FEM) has been extensively used for modeling flows in porous media.[11–14] Also available are several commercial software that can conduct fluid-flow simulations in porous media using FEM, such as PORFLOW, COMSOL, and ANSYS; these software can easily model the saturated, single-phase, flows in simple rigid porous substances, but none of them can incorporate the medium swelling effects in the flow modeling. Therefore, they cannot model flows in nonrigid, swelling porous media, such as those made of superabsorbent polymer, and cellulose fibers, such as paper towels, wipes, and paper napkins.

Correspondence concerning this article should be addressed to K. M. Pillai at krishna@uwm.edu
Current Address of: Reza Masoodi, School of Design and Engineering, Philadelphia University, 4201 Henry Ave Philadelphia PA 19144, USA.
Current Address of: Hua Tan, Engineering Modeling and Analysis Group, Hewlett-ackard Company, 1000 NE Circle Blvd, Corvallis, OR 97330.

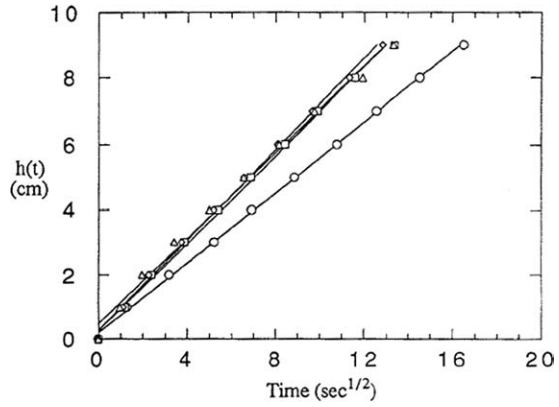

Figure 1. Wicking distance vs. square root of time for *n*-Octane. (○) 0% CMC; (□); 10% CMC; (◇) 20% CMC; (△) 30% CMC[7].

Note that, $h(t)$ corresponds to L_{lf} of our nomenclature. (This figure is replicated here with the kind permission of *Wood and Fiber Science*.)

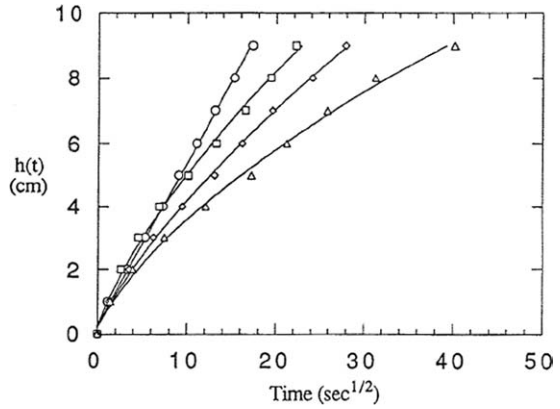

Figure 2. Wicking distance vs. square root of time for water. (○) 0% CMC; (□); 10% CMC; (◇) 20% CMC; (△) 30% CMC[7].

Here, $h(t)$ corresponds to L_{lf} of our nomenclature. (This figure is replicated here with the kind permission of *Wood and Fiber Science*.)

In this article, we are going to model a 2-D capillary-suction driven liquid flow in a porous network of cellulose fibers and powdered superabsorbents. PORE-FLOW©, a computer program developed in the Laboratory for Flow and Transport Studies in Porous Media at the University of Wisconsin-Milwaukee,[15] is used to solve the governing equations and conduct the flow simulation. PORE-FLOW© is a comprehensive computational fluid dynamics tool, focused primarily on solving the flow infiltration/wetting of porous media type problems. The finite element/control volume (FE/CV) method is implemented in the code to simulate single-phase flows behind a clearly observable moving-boundary.[16] The algorithm is efficient and robust for solving the moving-boundary problems in complex domain geometries.

The accuracy of estimated permeability is critical in calculating the flow and transport in porous media.[17] In this article, we describe a method to estimate the local permeability of a swelling matrix as a function of the wetting time, such that such a permeability function is later used to assign permeability to each element in our FE/CV simulation behind the moving liquid-front. The comparison of the numerical predictions and experimental data demonstrate the accuracy of our numerical simulation. The flow simulation is then used to predict the absorption rate in the swelling porous medium. We also suggest some ways of improving the permeability estimation to increase the accuracy of the numerical simulation.

Experimental Study

This research is based on an experimental study conducted at the University of Washington, where Wiryana and Berg[7] studied experimentally the wicking of water into paper strips consisting of cellulose fibers and different percentages of powdered carboxymethyl cellulose (CMC) superabsorbent. They used four different weight percentages of CMC (0, 10, 20, and 30%) in the paper stripes used in the wicking tests. To observe the swelling effect, they studied wicking with two different liquids: *n*-octane, as the reference nonswelling liquid, and water, as the swelling liquid.* The experiments showed no swelling in the matrix material while wicking *n*-octane, whereas there was considerable swelling while wicking water. They also observed that the swelling rate increased with the percentage of CMC. Figure 1 shows their wicking test results with *n*-octane—the linearity of the curves proves that there is no swelling with *n*-octane. Figure 2 shows the same tests with water—here, the nonlinear wicking curves indicate the swelling of the porous matrix; this nonlinearity increases with the percentage of CMC.†

Theory of Wicking

We assume that there is a clear liquid-front during wicking in the test material.‡ (Clear liquid-front assumption is a good one in the case of wicking/imbibition of liquids in thin, paper-like materials. We can see such a phenomenon during the wetting of paper napkins, when a clear liquid-front is seen moving in the napkin when one end of the napkin is put in touch with a wetting liquid.) Hence, we apply the Darcy's law based model to predict the single-phase flow behind the liquid-front.[9] The Darcy's law, for the flow of a single liquid in an isotropic porous medium under isothermal conditions, is given as

$$\langle \vec{V} \rangle = -\frac{K}{\mu} \vec{\nabla} \langle P \rangle^f \tag{1}$$

where $\langle \vec{V} \rangle$ and $\langle P \rangle^f$ are the volume-averaged liquid velocity, and the pore-averaged modified pressure, respectively. K is the permeability of the porous medium and μ is the liquid viscosity.[2,18] The modified pressure P relates to the gravity-induced liquid pressure and the pore-averaged hydrodynamic pressure p in the porous medium through the expression

$$P = p + \rho g h \tag{2}$$

Note that, in general, the permeability is a function of both time and space in swelling materials. The other

*The term swelling liquid means that the liquid induces swelling in the considered porous material.

†Increasing the CMC percentage means increasing the percentage of the superabsorbent material, which swells rapidly when put in contact with water-based liquids.

‡Clear liquid-front means that there is a clear and sharp boundary between the wet matrix with 100% saturation, and the dry matrix with 0% saturation.

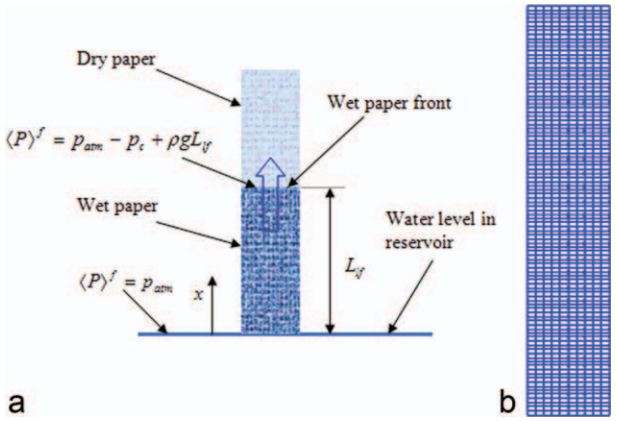

Figure 3. A schematic of the wicking setup and the fixed 2-D FE mesh used in the present numerical simulation.

(a) Wicking setup and boundary conditions and (b) 2-D mesh. [Color figure can be viewed in the online issue, which is available at wileyonlinelibrary.com.]

governing equation for the flow of an incompressible liquid in a porous medium is the macroscopic continuity or mass-balance equation. It was shown previously,[1,2] that the modified continuity equation for swelling porous media is

$$\vec{\nabla}\cdot\langle\vec{V}\rangle = -S - \frac{\partial\varepsilon}{\partial t} \tag{3}$$

where S is the sink term, which is the rate of liquid absorption by solid phase in the porous medium, and ε is the porosity. It was postulated[2] that the sink term is directly proportional to the rate of change of the porosity, and hence the above equation simplifies to

$$\vec{\nabla}\cdot\langle\vec{\mathrm{V}}\rangle = (b-1)\frac{\partial\varepsilon}{\partial t} \tag{4}$$

It was shown that b, the constant of proportionality or the absorption coefficient, being very close to one satisfies the experimental results the best,[1,2] so we assume, $b = 1$ here. (This implies that the volumetric rate of liquid absorption is equal to the volumetric rate of solid-phase expansion.). As a result, the continuity equation, Eq. 4, simplifies to

$$\vec{\nabla}\cdot\langle\vec{\mathrm{V}}\rangle = 0 \tag{5}$$

If the liquid viscosity is considered to be a constant, then a combination of Eq. 1 with Eq. 5 leads to the following equation for the modified pressure

$$\vec{\nabla}\cdot(K\,\vec{\nabla}\langle P\rangle^f) = 0 \tag{6}$$

Based on Figure 3a, and considering Eq. 2 for the modified pressure, the pressure boundary-conditions for the above given pressure equation can be expressed as

$$\langle P\rangle^f(x=0) = p_{\mathrm{atm}} \tag{7a}$$

$$\langle P\rangle^f(x=L_{\mathrm{lf}}) = p_{\mathrm{atm}} - p_{\mathrm{c}} + \rho g L_{\mathrm{lf}} \tag{7b}$$

Note that, the relation between the front speed and the volume-averaged liquid velocity at the liquid-front[18] is given as

$$\vec{V}_{\mathrm{lf}} = \frac{\langle\vec{V}\rangle}{\varepsilon}\cdot\hat{n} \tag{8}$$

On solving Eq. 6, the pressure field is determined, and then the application of Eq. 1 along with Eq. 8 gives the liquid-front velocity. After knowing the liquid-front velocity, one can easily find the liquid-front location. As permeability is a function of both time and space in swelling porous materials, so finding an analytical solution for Eq. 6 is very difficult, and hence a numerical solution will be sought.

Numerical Simulation

We used PORE-FLOW© for numerically modeling the capillary-suction driven liquid flow in swelling porous media behind a clear liquid-front. In the algorithm used by PORE-FLOW©, the transient fluid-flow in porous medium involving a moving-boundary (i.e., a flow front) is divided into multiple time steps. After assuming a quasi-steady condition during each time step, Eq. 6 is first solved for the modified pressure using the hybrid FE/CV algorithm in the wet region saturated by the moving liquid-front. Then, the pressure field computed at FE nodes using the Galerkin weighted residual method in conjunction with the boundary conditions of Eqs. 7a and 7b[§] is used to estimate the velocity field through Eq. 1 at the surfaces of CVs described around FE nodes; later, the velocity field is used to find the new location of the liquid-front at each time-step.

Note that, as the flow is essentially 1-D in our problem, a 2-D flow simulation is enough to capture the fluid flow in the considered 2-D flat plate geometry of the paper strips (see Figure 3b). The only difficulty here is the dependence of permeability in the wetted region behind the flow-front on time and space due to swelling of the porous matrix. Hence, the permeability of each element in the FE mesh used for the simulation is needed. Note that, the permeability of an element is a function of the local porosity, which in turn depends solely on the time that has elapsed since the wetting of the local solid phase. Therefore, the permeability is a function of time[¶] in each element. We need to find this generic permeability function for the FEs.

Permeability of an element, before it gets "wet" and its matrix starts swelling, is defined as the initial permeability, K_0. Once the element has been passed by the liquid-front, and its matrix has been wetted, the matrix starts swelling and the porosity (defined as the ratio of the pore volume to the total volume) begins reducing, and consequently the permeability starts reducing with time. If t_{wet} is the time when an element gets wet by the moving liquid-front or the corresponding fill factor becomes unity,[**] then the following general formula holds for the permeability of each element

$$K_i = \begin{cases} K_0 & t < t_{\mathrm{wet}} \\ \mathrm{fn}(t - t_{\mathrm{wet}}) & t \geq t_{\mathrm{wet}} \end{cases} \tag{9}$$

[§]Further details on the PORE-FLOW© algorithms are given in Refs. [9] and [16].

[¶]The time here refers to the time, the element has been wetted since the passage of the liquid-front through it.

[**]When the control volume defined around a finite element node is dry or empty, the fill factor is "0"; when it is wet or filled, the fill factor is "1". (The fill factor is defined as the ratio of the local pore volume filled with the advancing liquid.[9])

Table 1. The Properties of Test Liquids[5]

Characteristic	Unit	Water	*n*-Octane
Viscosity, μ	Pa s	0.000911	0.000522
Surface Tension, γ	N/m	0.0723	0.0212
Contact Angle, θ	Degree	0	0

Wiryana and Berg measured the contact angle to be zero for both liquids.[7]

where fn is any experimentally determined function. The accuracy of the numerical predictions is highly dependent on the accuracy of the estimated K_i. In the following section, we will explain an approach to estimate this parameter from the experimental results published by Wiryana and Berg.[7]

Estimating the wicking parameters

To solve the pressure equation, Eq. 6, we need the permeability of the porous medium and the capillary (suction) pressure at the liquid-front. The capillary pressure, p_c, is obtained through the well-known Young–Laplace equation[19] as

$$p_c = \frac{2\gamma\cos(\theta)}{R_c} \tag{10}$$

where R_c is the capillary radius, γ is the surface tension, and θ is the contact angle.[19] (The properties of the liquids used in the experiment are given in Table 1.) To estimate the capillary radius, we used the Lucas–Washburn equation[3,4] which gives the liquid-front location as the function of time for wicking of a ''nonswelling'' liquid, such as *n*-octane in a 1-D porous medium as

$$L_{lf} = \sqrt{\frac{\gamma R_c\cos(\theta)}{2\mu}}\sqrt{t} \tag{11}$$

Therefore, if we measure the slope of the fitted lines $h(t)$ vs. $t^{1/2}$ in Figure 1, it should be equal to $\sqrt{\frac{\gamma R_c\cos(\theta)}{2\mu}}$. As every parameter except R_c in this expression is known, therefore, one can calculate the capillary radius R_c.[††] The obtained results are presented in Table 2.

To estimate the permeability, we can use the same approach after using the Darcy's law based formulation for wicking. On assuming the paper stripes to be porous media, we can write the following expression[1] for the wicking tests shown in Figure 1.

$$L_{lf} = \sqrt{\frac{4K_0\gamma\cos(\theta)}{\varepsilon_0\mu R_c}}\sqrt{t} \tag{12}$$

Once again, we can use the measured slopes of the fitted lines in Figure 1 to find the values of $\sqrt{\frac{4K\gamma\cos(\theta)}{\varepsilon_0\mu R_c}}$. Here ε_0, the initial porosity is 0.59 for all materials. All other parameters in the expression are known, except the permeability K. As the test liquid in Figure 1 was *n*-octane, so the measured permeability should be equal to the initial permeability, K_0, as there were no swelling effects in the wicking tests with *n*-octane, and hence the porosity and consequently the permeability remain unchanged. The measured initial permeabilities are listed in Table 2.

[††]There is often a difference between the capillary radius and the hydraulic radius used in the Lucas–Washburn models for modeling wicking.[20]

Table 2. The Wicking Parameters for Test Specimens Estimated from Figure 1 Plots

% of CMC in test specimen	Capillary radius R_c (m)	Initial permeability K_0 (m^2)
0%	1.5 e −6	1.66 e −13
10%	2.47 e −6	4.51 e −13
20%	2.47 e −6	4.51 e −13
30%	2.47 e −6	4.51 e −13

Estimating changes in the local permeability

To make theoretical (analytic or numeric) predictions for the experimental wicking data showed in Figure 2, we should include the effects of matrix swelling by including a model for local change in the permeability with time in the theoretical models. The permeability and porosity of the paper-based porous medium reduces after wetting because the swelling of the solid (fiber) phase causes a decrease in the pore size, that is, an increase in fiber diameters causes a decrease in the surrounding pore space. If we use the method proposed by Masoodi and Pillai,[1] and use a global value for permeability,[‡‡] then the following equation can be used to predict the liquid-front location.

$$L_{lf} = \sqrt{\frac{2p_c}{\varepsilon_0\mu}\int_0^t K_{glob}(t')dt'} \tag{13}$$

If we use the time average of the global value of permeability within the integral and raise both the sides of the equation to a power of 2, then Eq. 13 simplifies to

$$L_{lf}^2 = \frac{2p_cK_{glob,\,ave}}{\varepsilon_0\mu}t \tag{14}$$

The use of Eq. 14 with the liquid-front vs. time experimental data given in Figure 2 yields different values for the global (average) permeability as a function of time. We used such linear equations as the best-fitted curves of L_{lf}^2 vs. t to find the varying global permeability, $K_{glob,ave}$, for different elapsed-times. Later, we used the measured global permeabilities, and used a regression technique to find the local permeabilities for equal liquid-front increments (i.e., the front locations at ΔL, $2\Delta L$, $3\Delta L$, …, $n\Delta L$ at times t_1, t_2, …, t_n, respectively). Then, these estimated permeabilities were used to estimate the permeability change in the first increment ΔL at different times. Following is a description of the method that was used.

At $t = 0$

The permeability is identical to the initial permeability of the nonswelled medium, that is, $K_{global} = K_0$.

From $t = 0$ to $t = t_1$:

We can use Eq. 14 to find the permeability of the first increment of length ΔL (see Figure 4a)

$$K_1 = \frac{\Delta L^2\varepsilon_0\mu}{2P_ct_1} \tag{15}$$

[‡‡]We propose two values for the permeability: the global permeability, which is the average permeability of the porous medium from the starting location of liquid wicking till the liquid-front location, and the local permeability, which is the permeability at each spatial location behind the front.

From $t = t_1$ to $t = t_2$:

Consider the Figure 4b for this time increment; the upper (second) part of length ΔL just got wet so its permeability is still K_1 (or $K_{\text{glob,ave}}$ $[t_1]$), but the permeability of the lower (first) part is unknown. The global permeability that we have estimated using the experimental data at time $t = t_2$ is $K_{\text{glob,ave}}(t_2)$. Now, we use the method explained in Appendix to calculate the permeability of the first part K_2 through the relation

$$\frac{\Delta L}{K_2} + \frac{\Delta L}{K_1} = \frac{2\Delta L}{K_{\text{glob,ave}}(t_2)} \tag{16}$$

Therefore, the permeability of the first part at this time interval will be

$$K_2 = 1/\left(\frac{2}{K_{\text{glob,ave}}(t_2)} - \frac{1}{K_1}\right) \tag{17}$$

From $t = t_2$ to $t = t_3$:

With a similar approach, we can find the permeability of the first part in the third time-interval (see Figure 4c) through the formula

$$\frac{\Delta L}{K_3} + \frac{2\Delta L}{K_{\text{glob,ave}}(t_2)} = \frac{3\Delta L}{K_{\text{glob,ave}}(t_3)} \tag{18}$$

Therefore, the permeability of the first part at this time interval will be

$$K_3 = 1/\left(\frac{3}{K_{\text{glob,ave}}(t_3)} - \frac{2}{K_{\text{glob,ave}}(t_2)}\right) \tag{19}$$

From $t = t_{n-1}$ to $t = t_n$:

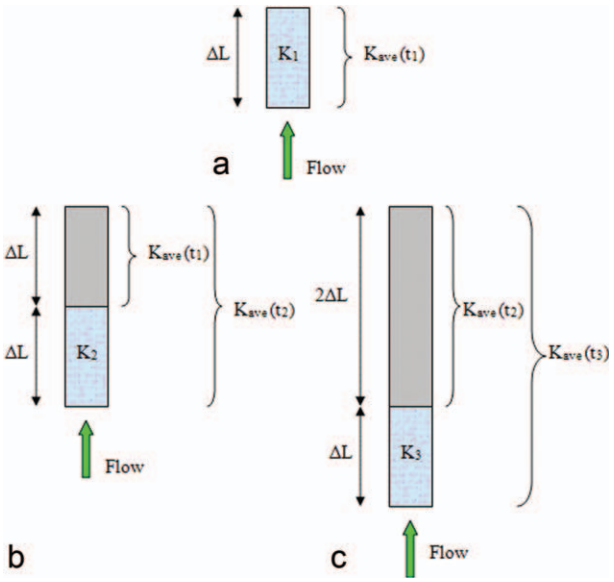

Figure 4. The permeabilities of the first part at times $t = t_1$ ($L_{lf} = \Delta L$), $t = t_2$ ($L_{lf} = 2\Delta L$), and $t = t_3$ ($L_{lf} = 3\Delta L$) along with the average permeabilities of the system.

(a) $t = t_1$, (b) $t = t_2$, and (c) $t = t_3$. [Color figure can be viewed in the online issue, which is available at wileyonlinelibrary.com.]

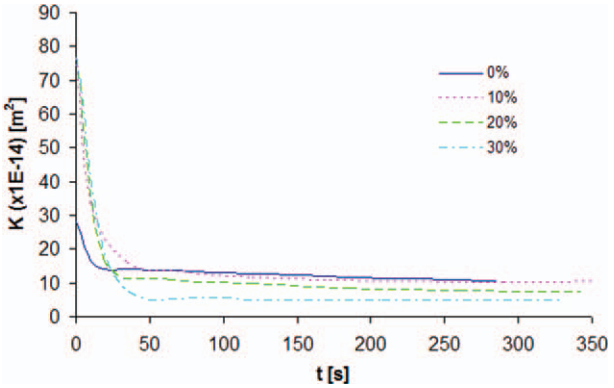

Figure 5. Estimated local permeabilities of different test materials (Eq. 21) as a function of time elapsed since the onset of wetting.

[Color figure can be viewed in the online issue, which is available at wileyonlinelibrary.com.]

Using the same approach as before, we get following expression for the permeability of the first part in the nth time interval.

$$K_n = 1/\left(\frac{n}{K_{\text{glob,ave}}(t_n)} - \frac{n-1}{K_{\text{glob,ave}}(t_{n-1})}\right) \tag{20}$$

The local permeabilities obtained from Eqs. 15 to 20 were assigned to various times to generate the plot of variation in the local permeability with time, that is, K_0 was assigned to $t = 0$, K_1 was assigned to $t = t_1/2$, K_2 was assigned to $t = (t_1 + t_1)/2$, K_n was assigned to $t = (t_{n-1} + t_n)/2$, and so on. Note that, the accuracy of estimated local permeability is related to the number of elements (n) in Eq. 20—to get accurate values for the local permeability, we have to use a large numbers of elements.

Figure 5 shows the local permeabilities estimated for different test materials. This local permeability change is assumed to be identical to the time-varying permeability of each element in the FE mesh after it gets wet by the invading flow-front. The best-fitting curve for the permeability variation with time t, as the onset of wetting was found to be of the form

$$K_{\text{loc}} = \left(\frac{A}{t+B} + C\right) \times 10^{-14} \tag{21}$$

where A, B, and C are the constant coefficients obtained through curve fitting techniques.[§§] The coefficient values for the three paper-like test materials are presented in Table 3. A comparison of the permeability estimated from the experimental data of Figure 2 using Eqs. 14–20, and the permeability predicted using the fitted curve Eq. 19 for the case of 20% CMC, is shown in Figure 6.

[§§]Note that, it is possible to find physical meanings for A, B, and C. Assume that the initial permeability before swelling is K_0, therefore, using Eq. 21 we have $K_0 = K_{\text{loc}}(@t = 0)$. If the ultimate value of permeability after complete swelling is K_∞, then $K_\infty = K_{\text{loc}}(@t \to \infty)$. Also assume the rate of permeability reduction at the beginning is λ [$\lambda = \frac{dK_{\text{loc}}}{dt}(@t = 0)$, that is, the initial slope of the K_{loc} vs. t plot or initial rate of permeability reduction due to swelling.]. If $\Delta K_{\text{loc}} = K_0 - K_\infty$ is the total reduction in permeability due to swelling, then we have the following expressions for the fitting parameters of Eq. 21, which gives physical meaning to each of the used parameters

$$A = \frac{\Delta K_{\text{loc}}^2}{\lambda}, \quad B = \frac{\Delta K_{\text{loc}}}{\lambda}, \quad C = K_\infty$$

Table 3. The Coefficients for Eq. 21 Obtained by Curve Fitting

% of CMC in test specimen	A	B	C
0%	45.8	4.7	6.8
10%	197.8	5.0	5.5
20%	147.0	3.6	3.7
30%	60.9	1.4	2.3

Results and Discussion

We have used PORE-FLOW©[15] to predict the wicking rate in the swelling, paper-like porous materials. The time-varying function found for the permeability, Eq. 21, provides continuous values for the permeability of any wetted element behind the liquid-front. After estimating the time-dependent permeability of the elements wetted by the liquid-front and the capillary suction pressure at the liquid-front, we were able to use PORE-FLOW© for numerical predictions. Note that, although the porosity of any swelling porous-medium is also varying as a result of the swelling and liquid absorption, but since there is no term involving porosity in the governing equations,¶¶ we did not model the changes in the porosity with time. The only porosity term that is needed is the initial porosity (i.e., the porosity before swelling), which is used to estimate the capillary suction pressure on the liquid-front. Note that, we assumed the porosity of the FEs at the liquid-front to be identical to the initial porosity of the test specimen, that is, the porosity of the dry medium before the onset of the swelling.

The numerically predicted contours of the pressure and liquid-front location, in a paper strip with 30% CMC, are shown in Figure 7. As the liquid movement is 1-D without any sink effect in the continuity equation (Eq. 4), therefore, we expect a linear pressure distribution; this is why we see constant distances between the contours in Figure 7a. The driving force is the capillary pressure, whereas the gravity "pressure" is against the liquid-front movement. As the liquid-front rises, the effect of gravity increases, and, therefore, the distance between the liquid-front contours in Figure 7b decreases with height.

Figure 8 compares the numerical predictions and experimental data for the test material with 0% CMC. Here, although the percentage of CMC or superabsorbent polymers is zero, we do have a slight swelling phenomenon because of the presence of cellulose fibers. Figure 8 shows that the numerical predictions are very accurate for this case, where the swelling rate is the minimum among considered the test samples.

Figure 9 shows the same comparison for the wicking tests with 10% CMC. Here, although the accuracy is still reasonable, it is not as good as in the previous figure. Figure 9 indicates that the accuracy of the numerical model is changing, and it reaches a minimum at $t = 100$ s; however, it is important to add that this maximum error is still less than 10%.

In Figure 10 for the case of 20% CMC, the trend is slightly different from the previous figures. Here, the accuracy decreases till $t = 80$ s and then starts to increase. From $t = 400$ s onwards, the accuracy is very good. Note that, the presence of 20% superabsorbent fibers results in a higher swelling rate compared to the previous experiments. As

¶¶As we assumed $b = 1$ in Eq. 4, so the porosity term was deleted from the right hand side of the continuity equation, Eq. 5.

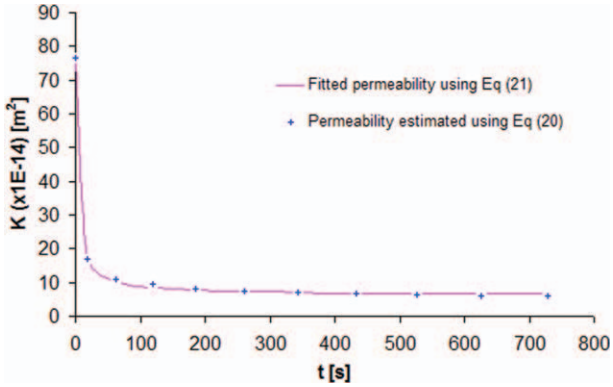

Figure 6. A comparison of the local permeabilities estimated through Eq. 20 and predicted using the fitted function Eq. 21 for a paper strip with 20% CMC.

[Color figure can be viewed in the online issue, which is available at wileyonlinelibrary.com.]

mentioned in the previous section, we used the curve-fitting procedures, while estimating the permeability functions for different materials. We believe that such fitting procedures caused slight error in wicking predictions as the fitted curves for estimated permeability may not match all the data points (see Figure 6).

The numerical predictions for wicking in the paper-like material with 30% CMC is shown in Figure 11. A rather good agreement between the experimental data and simulation is achieved. Note that, in this case, the highest percentage of superabsorbent material (30% of CMC) is present in the paper strip, and hence the highest rate of swelling occurred. Once again, there is still a slight error in the wicking predictions that can probably be attributed to the errors

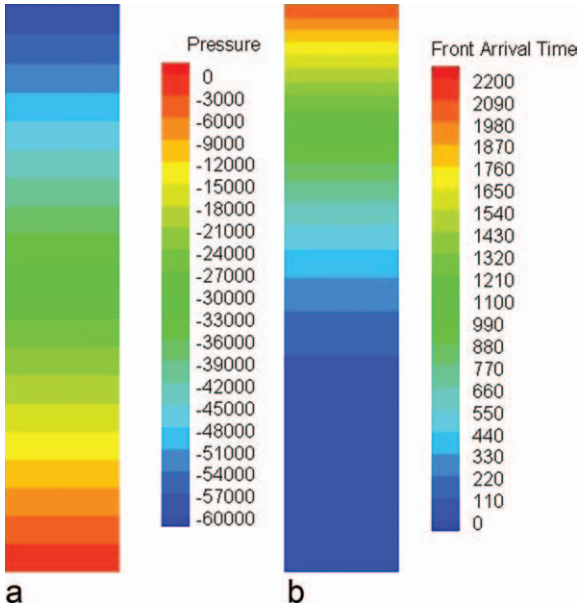

Figure 7. Typical contours of pressure and liquid-front progress, as predicted by the simulation in a paper strip with 30% CMC.

Note that, the pressure here is gage pressure ($P_{gage} = P_{absolute} - P_{atmosphere}$). (a) Pressure contours and (b) liquid-front contours. [Color figure can be viewed in the online issue, which is available at wileyonlinelibrary.com.]

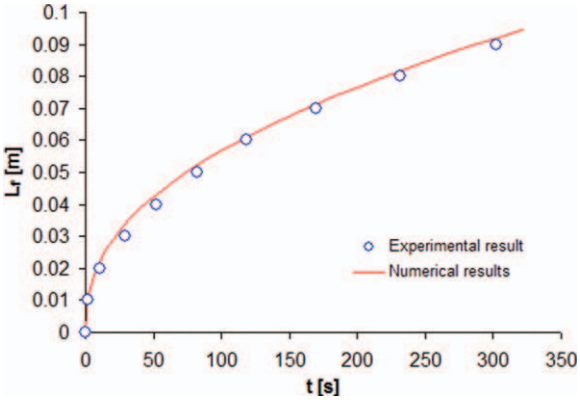

Figure 8. Comparing our numerical prediction with the reported experimental data for 0% CMC paper and superabsorbent polymer composite.

[Color figure can be viewed in the online issue, which is available at wileyonlinelibrary.com.]

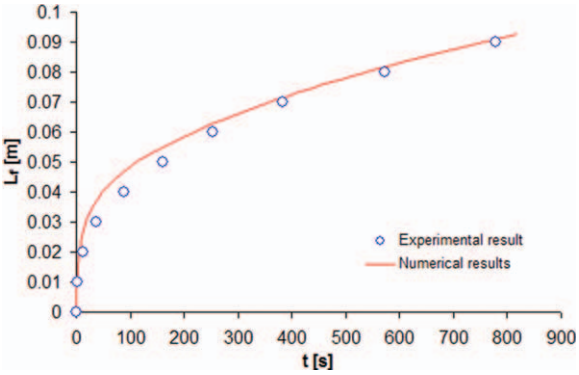

Figure 10. Comparing our numerical prediction with the reported experimental data for 20% CMC paper and superabsorbent polymer composite.

[Color figure can be viewed in the online issue, which is available at wileyonlinelibrary.com.]

arising from the curve fitting processes. However, the small error in the numerical prediction is insignificant and the proposed method should be considered as an excellent approach to make theoretical/numerical predictions.

The comparisons presented in Figures 8–11 establish the accuracy of our numerical simulation using PORE-FLOW© for predicting wicking in swelling, paper-like porous media. The slight differences between the experimental and numerical results in Figures 8–11 are perhaps due to the use of several assumptions and simplifications in our theoretical/numerical model. We would restate the three sets of assumptions and simplifications used in this study:

(1) Replacement of the transient permeability with an average permeability in Eq. 14.

(2) Use of regression functions to find the equal intervals for the wicking lengths in Eq. 20.

(3) Use of best-fitting curves while developing the local permeability functions in Eq. 21.

Use of these three assumptions and simplifications is likely to cause the above listed errors in the final wicking predictions, but the numerical results show that such errors are not significant. In future, attempts should be made to further reduce the errors accruing from the above assumptions. Using small time-steps in the wicking simulation improves the accuracy due to the first assumption. Using better fitting curves, such as the spline functions, can improve the accuracy due to the second assumption. The use of the experimental data file and the spline interpolations (instead of the mathematical relations) may improve the accuracy due to the third assumption.

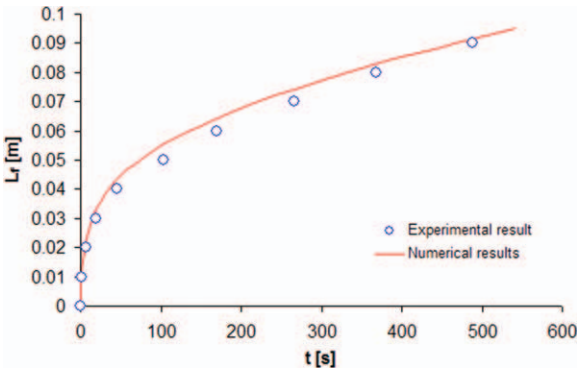

Figure 9. Comparing our numerical prediction with the reported experimental data for 10% CMC paper and superabsorbent polymer composite.

[Color figure can be viewed in the online issue, which is available at wileyonlinelibrary.com.]

Another explanation can be proffered regarding the deviations of the simulation from the experimental results. As we used the published experimental data which did not report the scatter in experimental observations, we did not have any information about the error bars. We contacted the corresponding author of Ref. [7] to see if he had any information on the scatter in his experimental data, but we did not get any new information other than published graphs. In this context, deviations between the simulation and the experimental results can also be explained due to inaccuracies in the experimental data.

As a final note on this topic of estimating prediction-errors, we would like to add that our theoretical model proposed through Eqs. 1–5 involves a fundamental assumption that the particles of a porous medium are fixed in space while undergoing swelling during the wicking process. In the cited work of Wiryana and Berg,[7] the swelling experiments were conducted with paper strips, where swelling would lead to an increase in the thickness of the strips,[***] and is likely to cause small displacements of the fibers constituting the porous medium. As a result, the use of the proposed flow model will incur a slight in-built error, however, small it may be.

Summary and Conclusions

The authors have proposed a novel theoretical model to predict the wicking in a swelling, liquid-absorbing porous medium. In this article, the numerical implementation of the model was validated against the previous published experimental data by Wiryana and Berg[7] on wicking in composite paper made of a network of cellulose fibers and different percentage of the superabsorbent CMC. Because of the swelling of matrix in such a porous medium, the porosity and permeability vary with time and space behind the moving liquid-front. We developed a novel technique to estimate the local permeability changes in swelling porous materials using the experimental data on wicking rate. The local

[***]No information on the changes in thickness of the paper strips used in their experiments was provided by Wiryana and Berg.[7]

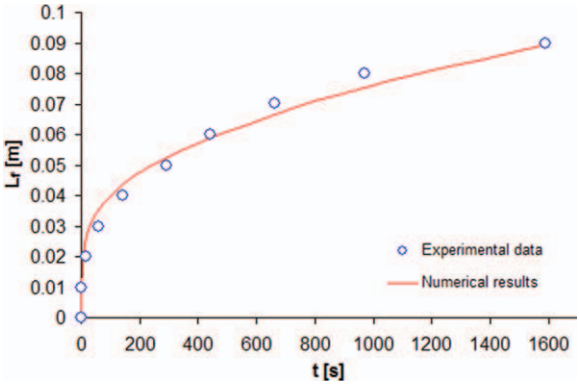

Figure 11. Comparing our numerical prediction with the reported experimental data for 30% CMC paper and superabsorbent polymer composite.

[Color figure can be viewed in the online issue, which is available at wileyonlinelibrary.com.]

permeability functions and the capillary suction-pressure expression were used to predict the wicking rate as a function of time using the computer program PORE-FLOW©.[15] It is important to add here that this is the first time such a simulation is used to model the liquid flow in a *swelling* porous medium during the wicking process. The numerical predictions in general compared well with the reported experimental data for 0, 10, 20, and 30% CMC in the superabsorbent-paper composite. Some ways to further improve the accuracy of numerical predictions through the use of improved fitting functions are also suggested. In general, this study demonstrated the efficacy of our numerical simulation based on the FE/CV algorithm and using a sharp liquid-front assumption in predicting the wicking rate in swelling porous media.

Notation

Roman letters

A = a constant coefficient (Eq. 21) sm^2
B = a constant coefficient (Eq. 21) s
b = absorption coefficient, 1/s (Eq. 4)
C = a constant coefficient (Eq. 21) m^2
fn = a general function (Eq. 9)
K = permeability, m_2
L = length, m
n = unit normal vector
P = modified pressure ($P = p + gh$), Pa
p = liquid pressure, Pa
R = radius, m
S = sink term in the modified continuity equation, 1/s
t = time, s
$\vec{V}$ = velocity vector, m/s
x = x-coordinate

Greek letters

θ = contact angle, degree
γ = surface tension of liquid, N/m
μ = viscosity of liquid, kg/m s
ε = porosity (dimensionless)
∇ = gradient operator
λ = the initial rate of local permeability reduction due to swelling

Superscripts

' = dummy variable
f = fluid or pore related

Subscripts

0 = initial value
1 = related to time interval $t = 0$ s to $t = t_1$ s (Eq. 15)
2 = related to time interval $t = t_1$ s to $t = t_2$ s (Eq. 17)
3 = related to time interval $t = t_2$ s to $t = t_3$ s (Eq. 19)
∞ = final value
atm = atmosphere
ave = average
c = capillary
glob = global value
i = element "i"
lf = liquid-front
loc = local value
n = related to time interval $t = t_{n-1}$ s to $t = t_n$ s (Eq. 20)
t = total
wet = wetting

Other symbols

$\langle\rangle$ = volume-averaged quantities (Eq. 1)
$\langle\rangle^f$ = pore-averaged quantities (Eq. 1)

Literature Cited

1. Masoodi R, Pillai KM. Darcy's law based model for wicking in paper-like swelling porous media. *AIChE J*. 2010;56:2257–2267.
2. Masoodi R. Modeling imbibition of liquids into rigid and swelling porous media. PhD Thesis, Dept. of Mechanical Engineering, University of Wisconsin, Milwaukee, 2010.
3. Lucas R. Rate of capillary ascension of liquids. *Kollid Z*. 1918;23:15–22.
4. Washburn EV. The dynamics of capillary flow. *Phys Rev*. 1921;17:273–283.
5. Schuchardt DR. The effects of fiber swelling on liquid transport in fibrous media. MS Thesis, Department of Chemical Engineering, University of Washington, Seattle, 1989.
6. Schuchardt DR, Berg JC. Liquid transport in composite cellulose superabsorbent fiber network. *Wood Fiber Sci*. 1990;23:342–357.
7. Wiryana S, Berg JC. The transport of water in wet-formed networks of cellulose fibers and powdered superabsorbent. *Wood Fiber Sci*. 1991;23:456–464.
8. Masoodi R, Pillai KM, Varanasi PP. Darcy's law based models for liquid absorption in polymer wicks. *AIChE J*. 2007;53:2769–2782.
9. Masoodi R, Tan H, Pillai KM. Darcy's law based numerical simulation for modeling 3-D liquid absorption into porous wicks. *AIChE J*. 2011;57:1132–1143.
10. Bear J. *Dynamics of Fluids in Porous Media*. American: Elsevier Science, 1972; pp. 270–271.
11. Chen Z, Huan G, Ma Y. *Computational Methods for Multiphase Flows in Porous Media*. Philadelphia: Society for Industrial and Applied Mathematics, 2006.
12. Tan H, Pillai KM. Numerical simulation of reactive flow in liquid composite molding using flux-corrected transport (FCT) based finite element/control volume (FE/CV) method. *Int J Heat Mass Transfer*. 2010;53:2256–2271.
13. Tan H, Pillai KP. Finite element implementation of stress-jump and stress-continuity conditions at porous-medium, clear-fluid interface. *Comput Fluids*. 2009;38:1118–1131.
14. Tan H, Pillai KP. Effect of fiber-mat anisotropy on 1D mold filling in LCM: a numerical investigation. *Polym Compos*. 2008;29:869–882.
15. PORE-FLOW©: A computer program developed at University of Wisconsin-Milwaukee to model fluid motion in porous media using the FE/CV filling algorithm. Available at: http://www4.uwm.edu/porous/
16. Tan H. Simulation of flow in dual-scale porous media. PhD Thesis, Dept. of Mechanical Engineering, University of Wisconsin, Milwaukee, 2010.
17. Vechart A, Masoodi R, Pillai KM. Design and evaluation of an idealized porous medium for calibration of permeability measuring devices. *Adv Compos Lett*. 2010;19:35–49.
18. Tucker CL, Dessenberger RB. *Governing equation for flow and heat transfer in stationary fiber beds*. In: Advani SG, editor. *Flow and Rheology in Polymer Composites Manufacturing*. Amsterdam: Elsevier, 1994; Chapter 8.
19. Masoodi R, Pillai KM. A general formula for capillary suction pressure in different porous media. will appear in *J Porous Media*. 2012;15.

20. Masoodi R, Pillai KM, Varanasi PP. Role of hydraulic and capillary radii in improving the effectiveness of capillary model in wicking. ASME Summer Conference, Jacksonville, FL, USA, August 10–14, 2008.

Appendix

Permeability of a Hybrid System

A hybrid porous system is a porous medium consists of different porous media. Let us consider a hybrid system of two porous media with identical cross-sections, and which are connected in series (see Figure A1). Here, the relevant length and permeabilities of two porous media are L_1, L_2, K_1, and K_2. If L_t and K_t are the total length and total permeability of the system, then

$$L_1 + L_2 = L_t \tag{A1}$$

Let us now find the relation between the permeability of the system, K_t, and the permeabilities of its consisting parts, K_1 and K_2. On the basis of Darcy's law, we have following expression for the hybrid system

$$Q = \frac{K_t}{\mu}\frac{\Delta P_t}{L_t} \tag{A2}$$

where Q is the Darcy velocity (flow rate per unit area) and ΔP_t is the steady-state pressure drop occurring in the hybrid system. As the Darcy velocities within each porous media and the hybrid system are the same, so

$$Q = \frac{K_1}{\mu}\frac{\Delta P_1}{L_1} = \frac{K_2}{\mu}\frac{\Delta P_2}{L_2} \tag{A3}$$

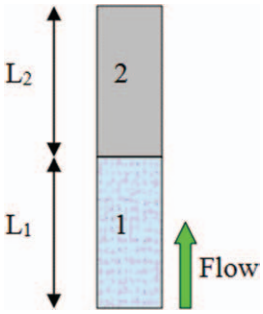

Figure A1. A schematic of a simple hybrid system consisting of two porous media arranged in series.

[Color figure can be viewed in the online issue, which is available at wileyonlinelibrary.com.]

Note that, the total pressure drop is equal to the sum of the individual pressure-drops in both the media

$$\Delta P_1 + \Delta P_2 = \Delta P_t \tag{A4}$$

If the pressure-drop expressions from Eqs. A2 and A3 are put into Eq. A4, we get

$$\frac{L_1}{K_1} + \frac{L_2}{K_2} = \frac{L_t}{K_t} \tag{A5}$$

So, the overall hybrid permeability K_t is the harmonic mean of the two constituent permeabilities, K_1 and K_2.

Manuscript received Dec. 22, 2010, revision received Jun. 9, 2011, and final revision received Aug. 17, 2011.